Alterations of the neural code in Parkinson's disease: a GPi simulation study

Daniela S. Andres[†‡*] , Florian Gomez[†] and Ruedi Stoop[†]

†Institute of Neuroinformatics, ETH Zurich and University of Zurich
Winterthurerstrasse 190, CH-8057 Zurich, Switzerland
‡Institute for Neurological Research Raul Carrea, Fleni Institute,
Movement Disorders Section, Buenos Aires, Argentine
* Society in Science, The Branco-Weiss Fellowship, administered by ETH, Zurich, Switzerland
Email: dandres@ini.uzh.ch, fgomez@ini.phys.ethz.ch, ruedi@ini.phys.ethz.ch

Abstract– Parkinson's disease is a movement disorder characterized by alterations in the neuronal activity of the Basal Ganglia. In healthy conditions, neurons of the Globus Pallidus pars interna (GPi - one of the main output centers of the Basal Ganglia network) use at least partly a rate-code to transmit information to the motor cortex. Applying a temporal structure function analysis, we measured the rate-coding window in single Globus Pallidus pars interna (GPi) neurons of the 6-OHDA rat model of Parkinson's disease at different degrees of alertness, and compared it to non-parkinsonian control neurons. We found that the temporal range of rate-coded information in GPi neurons was substantially reduced in the parkinsonian case. Making use of a network of coupled non-linear neurons, we model the GPi and show that the rate-code loss can be attributed to an increase in the small neighborhood coupling strength.

1. Introduction

Parkinson's disease (PD) is a neurodegenerative disorder, marked by the loss of dopamine in the Basal Ganglia (BG) [1]. Currently, the main explanatory framework accounting for the pathophysiology of PD is the so called classic model. It offers an interpretation of PD based on the overactivity of the output structures of the BG, namely the GPi and the Substantia Nigra pars reticulata (SNr - for a summary of the circuit alterations occurring in PD, see fig. 1) [2, 3]. These output centers are connected with an inhibitory projection to the motor Thalamus (Th), and therefore their effect is considered to be anti-kinetic (impairing voluntary movement). This anti-kinetic activity is stimulated through the indirect pathway of the BG, and inhibited through the direct pathway (considered anti-kinetic and pro-kinetic, respectively). The effect of dopamine, which is progressively lost in PD, is to reduce the anti-kinetic activity by exerting a stimulatory effect over the direct pathway and an inhibitory one over the indirect pathway of the BG circuit [4].

A number of pathologic changes in the activity of BG neurons have been shown to present a correlation with the clinical manifestations of PD [5]. Of particular interest are the alterations in the activity of the Globus Pallidus pars interna (GPi), one of the main output centers of the BG network, since its high frequency stimulation with deep brain electrodes is able to reduce the symptoms of the disease [6]. The principal pathologic changes in the activity of the GPi in PD are: 1. an increase in the frequency of discharge, and 2. enhanced synchronization of the neuronal activity [1, 7]. In a previous work by our group, we showed that the rate-coding window of single GPi neurons is reduced in an animal model of PD, applying a structure function analysis to the comparison between neuronal recordings from a control group and a group of parkinsonian Sprague-Dawley, adult rats [8]. Here, we discuss a non-linear model of the GPi and analyze the changes that occur in the rate-coding window of single neurons following the increase of the local coupling strength.

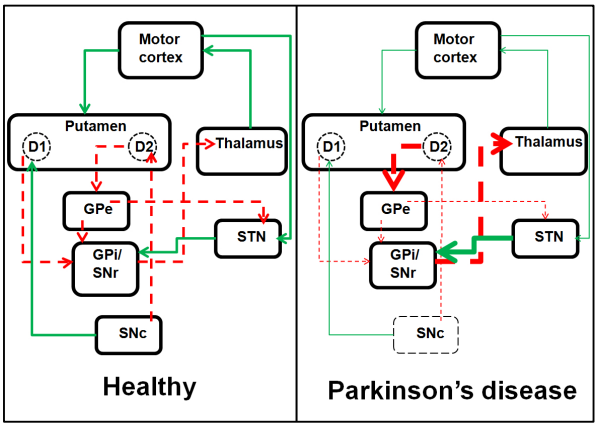

Figure 1. Main pathways of the Basal Ganglia network in healthy conditions and in Parkinson's disease. GPe: Globus Pallidus pars externa, GPi: Globus Pallidus pars interna, SNr: Substantia Nigra pars reticulata, SNc: Substantia Nigra pars compacta, STN: subthalamic nucleus, D1 / D2: dopamine receptors subfamilies. Red-dotted arrows represent inhibitory connections, and green-solid arrows excitatory ones. The thickness of the arrow represents the strength of the connection. In Parkinson's disease the SNc (the origin of dopamine) is progressively degenerated due to cell death.

2. Methods

2.1. Structure function analysis

Identifying different states of a system according to its different scaling behaviors can be a key to the study of complex systems based on time series analysis [9]. To this

goal, a method that has been shown to be robust to the presence of drift, low frequency noise and short time series is the structure function analysis [10-12]. To analyze the temporal organization of single neurons' activity, the temporal structure function can be calculated based on an interspike interval (ISI) time series, where $I(j)$ is the jth interspike interval and $\Delta I(\tau) = I(j+\tau) - I(j)$ is the difference between successive intervals, separated by an index increment $\tau \in N+$. The structure function $S_q(\tau)$ is defined as

$$S_q(\tau) = \left\langle \left| \Delta i(\tau)^q \right| \right\rangle \quad , \tag{1}$$

where $\langle \cdot \rangle$ accounts for the statistical average over the time series and q is a real number. The scaling behavior of S_q is then characterized by the power law relationship

$$S_q(\tau) \sim \tau^{\zeta(q)} \quad . \tag{2}$$

For a stationary process with independent increments $\zeta(q) = 0$, which expresses that the mean correlation between successive events does not depend on the event index [13]. Monofractal, non-intermittent time series imply $\zeta(q) = const$, whereas multifractal behavior is characterized by $\zeta''(q) < 0$. Therefore, the zero-slope regime ($\zeta(q) = 0$) of the structure function is of particular interest, since it marks the temporal scale across which only random processes are at work. For neuronal signals, this regime precludes coding schemes other than a rate code. Therefore, the zero-slope regime can be assimilated to the temporal window of rate-coding.

2.2. Mathematical model

We build a network in the form of a ring of coupled nonlinear Rulkov neurons [14]. The network architecture was considered identical for both the PD and the control case. In total, 101 GPi neurons were implemented, aligned on a ring structure. The inputs of the subthalamic nucleus (STN) and Striatum (Str) to the GPi are modeled as excitatory and inhibitory inputs respectively, and the spatial distribution of both inputs is close to the available histological data [15]. Excitatory input to the GPi is mediated by 101 STN axons, each of which sends collaterals to 10 neighboring cells using identical synaptic weights (wSTN-GPi=0.1). Inhibitory input to the GPi is mediated by 101 Str axons producing 10 collaterals each: one central connection to a GPi neuron with a high synaptic weight (wStr-GPi-I=0.9) and 9 connections to adjacent cells with a lower weight (wStr-GPi-II=0.01). In the simulation, each neuron has the form

$$x_{i,n+1} = f(x_{i,n}, y_{i,n} + \beta_{i,n}) \quad , \tag{3}$$

$$y_{i,n+1} = y_{i,n} - \mu(x_{i,n} + 1) + \mu\sigma + \mu\sigma_{i,n} \quad , \tag{4}$$

where the index n indicates the iteration step, and where function f is given by

$$f(x_n, y) = \begin{cases} \alpha/(1-x_n) + y, & x_n \le 0 \\ \alpha + y, & 0 < x_n < \alpha + y \quad and \quad x_{n-1} \le 0 \\ -1, & x_n \ge \alpha + y \quad or \quad x_{n-1} > 0 \end{cases} . \tag{5}$$

External input was modeled by

$$\sigma = \sigma_u + I_c \ , \tag{7}$$

where σ_u represents the initial excitability of each isolated neuron and I_c models the input to the cell. Inputs were modeled by uniformly distributed random numbers from the unit interval, multiplied by the amplitude A_e, for excitatory input or by amplitude A_i, for inhibitory input, respectively. For every neuron, the parameter values $\alpha = 4.5$ and $\mu = 0.001$ were used. To account for variability in initial neuronal excitation, σ_u was drawn uniformly from [0.05, 0.15]. Small-range interactions were modeled by diffusive coupling among GPi cells. The coupling from each neuron i to its neighbors is described by the following equations (cf. [14], where we set β_e and σ_e to 1):

$$\beta_{i,n} = g_{ji} \beta^e (x_{j,n} - x_{i,n}) \quad , \tag{8}$$

$$\sigma_{i,n} = g_{ji} \beta^e (x_{j,n} - x_{i,n}) \quad , \tag{9}$$

The local dependence of the coupling on the neighbor order j was implemented by

$$g_{ji} = \frac{D}{\left| (i-j) \right|^2} \ . \tag{10}$$

Here, g_{ji} are the elements of the adjacency matrix, which is symmetric assuming periodic boundary conditions, according to eq. 10. This form of coupling implies that the coupling strength decreases following a power-law with

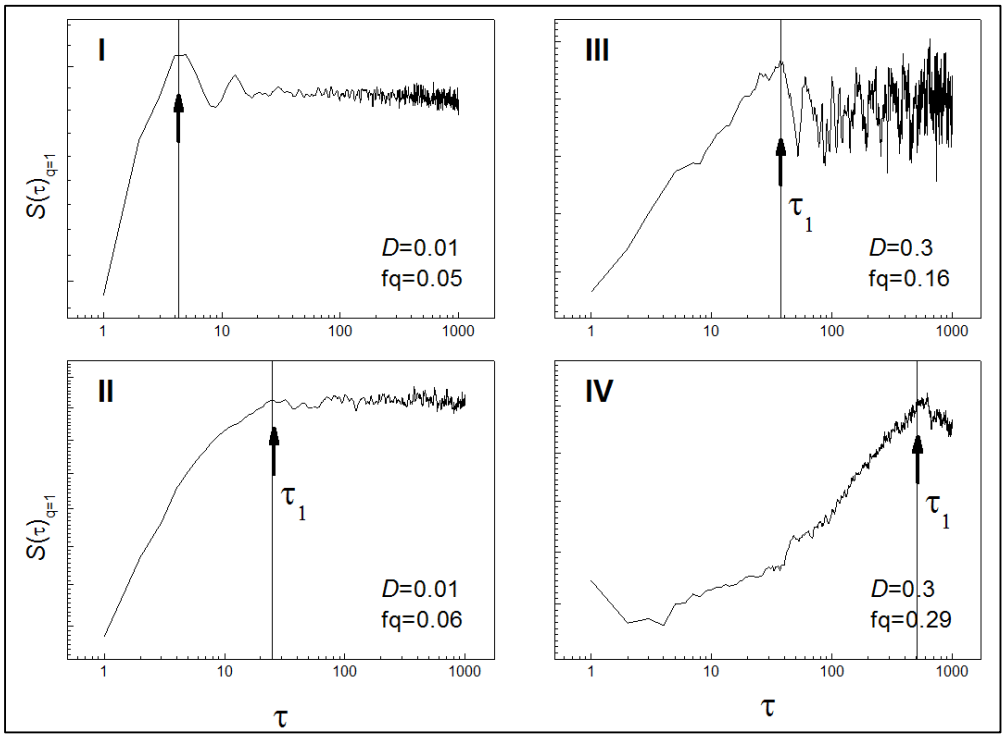

Figure 2. Order-1 structure functions of the four simulated groups. A), B) Deep anesthesia condition, control and PD case, respectively. C), D) Full alertness condition, control and PD case, respectively. Smoothing over 20 data points was applied to the original data. Arrows indicate the breakpoint τ_1 , where the small scale regime ends. Control neurons show a clear zero-slope scale-range (regime II) at both alertness conditions. PD neurons do not always show such a region. In the PD case neurons have an increased τ_1 compared to the control group.

the lattice distance, and hence D can be assimilated generally to a diffusion coefficient.

We based our modeling on experimental data from previous works, and studied the parkinsonian and control case under 2 conditions: anesthetized and at full alertness. We modeled the parkinsonian case introducing a stronger diffusion constant (D=0.3 in the PD vs. D=0.01 in the control case) in addition to differing excitatory / inhibitory input levels (in agreement with the classic model of PD). The distinction between anesthetized and alert conditions was modeled by changed input amplitudes (Andres et al. 2014). Whereas the anesthetized condition was modeled by A_e=1.5/25 and A_i=-1.2/-24.5, the alert condition was modeled by A_e =2/50 and A_i=-1.5/-48.5 (control / PD cases, respectively). In this way, the two conditions were characterized by slightly different A_e/A_i ratios of 1.25/1.02 (anesthesia) and 1.33/1.03 (alertness) for the control / PD case, respectively. (For details on our experimental data, see [16]).

3. Results

In our simulations, the PD case had a frequency of discharge significantly higher than the control case, which resembles the experimental situation. In the temporal structure function, two main regimes were identified. Regime I referred to the small-scale regime and showed an ascending behavior, ending abruptly at the breakpoint that we named τ_1. This was followed by regime II, which corresponded to an essentially flat region. As was stated above, this flat region of the structure function represents the rate-coding window of the neuronal activity, and this regime was reduced in the PD simulation. The breakpoint τ_1 moved further to the right from the control case under deep anesthesia (group I), to the control case at full alertness (group II) and the PD case under anesthesia (group III), and was highest in the PD case at full alertness (group IV). This marked the progressive reduction of the zero-slope scale-range, indicating a loss of the rate-coding properties in PD neurons.

4. Discussion and conclusion

In the parkinsonian BG, experimental evidence has shown that the frequency of discharge of GPi neurons is increased, and that the neuronal activity within the nucleus is pathologically synchronized [17]. None of these observations, however, provide any insight about the organization of the neuronal discharge in the time-domain. Applying a temporal structure functions analysis, we showed that different time scales are present in the activity of GPi neurons. This speaks in favor of a multiple-scale instead of a scale-free temporal

organization of the neuronal discharge, implying that the transmission of information might be favored in a limited time-range. In the GPi, Parkinson's disease acts deteriorating these temporal scales that are characteristic of healthy neuronal activity. We modeled this situation introducing diffusive coupling in a network of non-linear Rulkov neurons. This form of coupling shows a dependence on distance, and we hypothesize that this is necessary due to physiological processes involved in neuronal coupling other than synaptic cell-to-cell connectivity [18, 19].

Acknowledgments

We would like to thank the technical personnel at the Institute of Neuroinformatics, ETH and UZH, Zürich, Switzerland, and at the laboratories of the Center for Applied Neurological Research, Fleni Institute, Buenos Aires, Argentine, who helped making this work possible. The work at Federal University of Parana, Curitiba, Brazil, was possible by financial support from following Brazilian government agencies: CNPq and CAPES.

References

[1] J. A. Obeso, M.C. Rodríguez-Oroz, M. Rodríguez, J. L. Lanciego, J. Artieda, N. Gonzalo, W. Olanow, "Pathophysiology of the basal ganglia in Parkinson's disease", *Trends in Neuroscience*, 23(Suppl.), pp.S8-S19, 2000.

[2] R. L. Albin, A. Young, J. B. Penny, "The functions anatomy of basal ganglia disorders", *Trends in Neuroscence*, 12, pp.366–75, 1989.

[3] M. R. DeLong, "Primate models of movement disorders of basal ganglia origin", *Trends in Neuroscence*, 13, pp.281–5, 1990.

[4] C. R. Gerfen, D. J. Surmeier, "Modulation of Striatal Projection Systems by Dopamine", *Annual Review of Neuroscience*, 34, pp.441-466, 2011.

[5] A. Galvan, T. Wichmann, "Pathophysiology of parkinsonism", *Clinical Neurophysiology*, 119, pp.1459-1474, 2008.

[6] A. Albanese, L. Romito, "Deep brain stimulation for Parkinson's disease: where do we stand?" *Frontiers in Neurology*, doi:10.3389/fneur.2011.00033, 2011.

[7] C. Hammond, H. Bergman, P. Brown, "Pathological synchronization in Parkinson's disease: networks, models and treatments", *Trends in neuroscience*, 30(7), pp.357-364, 2007.

[8] D. S. Andres, F. Gomez, D. Cerquetti, M. Merello, R. Stoop, "A hierarchical coding-window model of Parkinson's disease", *Lecture Notes on Computer Science*, in press, 2014.

[9] K. Hu, P. C. Ivanov, Z. Chen, P. Carpena, E. Stanley, "Effect of trends on detrended fluctuation analysis", *Physical Review E*, 64(1):011114, 2001.

[10] U. Frisch, *Turbulence, The legacy of A.N. Kolmogorov*, Cambridge, University Press, 1996.

[11] R. Benzi, S. Ciliberto, R. Tripiccione, C. Baudet, F. Massaioli, S. Succi, "Extended self-similarity in turbulent flows", *Physical Review E*, 48(1), pp.R29-R32, 1993.

[12] E. O. Schuls-DuBois, I. Rehberg, "Structure function in Lieu of correlation function", *Applied Physics*, 24, pp.323-329, 1981.

[13] S.I. Vainshtein, K.R. Sreenivasan, R.T. Pierrehumbert, V. Kashyap, A. Juneja, "Scaling exponents for turbulence and other random processes and their relationships with multifractal structure", *Physical Review E*, 50(3), pp.1823-1835, 1994.

[14] N. F. Rulkov, "Modeling of spiking-bursting neural behavior using two-dimensional map", *Physical Review E*, 65: 041922, 2002.

[15] M. Difiglia, J. A. Rafols, "Synaptic organization of the Globus Pallidus", *Journal of Electron Microscopy Technique*, 10: 247-263, 1988.

[16] D. S. Andres, D. Cerquetti, M. Merello, R. Stoop, "Neuronal entropy depends on the level of alertness in the parkinsonian Globus Pallidus in vivo", *Frontiers in Neurology*, doi: 10.3389/fneur.2014.00096, 2014.

[17] J. Dostrovsky, H. Bergman, "Oscillatory activity in the basal ganglia – relationship to normal physiology and pathophysiology", *Brain*, 127, pp.721-722, 2004.

[18] R. L. Viana, J. C. A. de Pontes, S. R. Lopes, C. A. S. Batista, A. M. Batista, "Controlling chaotic bursting in map-based neuron network models", in C. Grebogi and M. A. F. Sanjuán (Eds.), *Recent Progresses in Controlling Chaos, Series on Stability Vibration and Control of Systems*, Series B - Vol. 16 , Chapter 10. Singapore: World Scientific, 2010.

[19] C. A. Anastassiou, R. Perin, H. Markram, C. Koch, "Ephaptic coupling of cortical neurons", *Nature neuroscience*, doi:10.1038/nn.2727, 2011.